ISSN No:-2456-2165

Bathymetric Information and Shoreline Delineation along Anyaogologo River, Rivers State, Nigeria

eke, stanley Nwaudo & Jonah, IYOWUNA benjamin
Rivers State University, Port Harcourt
Department of Surveying and Geomatics

Abstract:- Shoreline mapping, determination of itsdeterioration and bathymetry overtime resulting from the socio-economic activities are of high importance. Satellite remote sensing offers an alternative to conventional topographic mapping and hydrographic surveys for measuring the extent of Land Use-Land cover changes and water depth, with the advantage of low cost and large area coverage. The use of multi –spectral image of Spot-5 and Landsat ETM7+ with high resolution provides possibility for shoreline variation and bathymetry mapping. This study mapped and analyzed variations along the Eagle Island Shoreline from the year 1986 to 2015 using Landsat ETM-7+ and Spot-5 imageries. The images were pre-processed and classified using ENVI 4.5 software and ArcGIS 10.0 software, while Surfer 10.0 was used for the 3-D modeling of the Echo sounding in situ measurement. The Midas Echo sounder was used for in situ measurement of the depth of the study area. The result showed a shoreline decrease of 1000 square meters from 2,745,000 square meters in 1986 to 1,457,731 square meters in 2015. The area occupied by water body decreased from 594,900 square meters to 440,918.75 square meters that's an increase of 400,000 square meters that is 40%, the built-up area increased from 1,001,700 square meters in 1986 to 1,401,575 square meters in 2015. The lengths of the shoreline for the various years were found to be 3.761 kilometer in 1986, 3.832 kilometers in 2000, and 3.743 kilometers in 2015, showing a decrease of 18m in 30 years. The study demonstrated the relevance of satellite imagery in mapping shoreline changes and the use of echo sounding technique in determining depth useful for navigational decision making. Regular shoreline mapping is recommended to avoid costly structure placement along shorelines, shoreline mapping aids in better boundary definition among communities near shorelines, and better-quality images free of cloud cover and haze would allow for a more accurate assessment of bathymetry, potentially removing the majority of error affecting classification methods, according to the study.

I. INTRODUCTION

Mapping coastal or shoreline bathymetry has been a key component of geographical application work for two reasons: one, to collect information on the state of the seabed for academic purposes, and the other, to collect data for management purposes. Bathymetry is becoming more important in a variety of marine applications, including marine navigation, oil and gas exploration, and the development of harbours. Despite the fact that water covers 71% of the Earth's surface, its oceans, seas, and other water bodies are inadequately mapped. The majority of the world's cities with larger populations are situated near a coastline. According to (Wong et al, 2007), 39 of the world's 39 capital cities with populations of more than 5 million people are within 100 kilometers of the coast. As a result, bathymetric data is becoming increasingly important in sectors like nautical maritime navigation and coastal planning and management. Remote sensing photography is becoming more prevalent in the study of underwater characteristics, and as a result, bathymetric applications are becoming more relevant. Remote sensing can be divided into two categories: passive and active. Thermal, multi-spectral, and hyper-spectral imagery are produced using the passive approach of remote sensing, which uses sensors to monitor the electromagnetic radiation reflected by the object. The active technique of remote sensing, on the other hand, necessitates the emission of energy in order to measure the resulting reflection. Active sensors include things like lidar, radar, and sonar. Using echo sounding and hydrographic survey techniques to map shallow coastal waters (shoreline) is expensive, time-consuming, and limited. Fortunately, remote sensing provides an alternative method by assessing the reflectance of optical bands, which is highly correlated with water depth.

A. Aim of the Study

The aim of this study is to map and analyse the changes along the Eagle Island shoreline from the year 1986 to 2015 using High resolution satellite imagery.

B. Objectives

To achieve the above aim, the following objectives were considered:

- To determine shoreline variation over the years using spot-5 and Landsat TM-7 Satellite imagery.
- To determine bathymetric depth of the shoreline using Echo sound field data.
- To produce the map of the Eagle Island Shoreline.

ISSN No:-2456-2165

C. Study Area

The Eagle Island is located in the Nkpolu-Oroworukwo area of Diobu, to the south of Port Harcourt, and is bordered on the north by the Rivers State University of Science and Technology. The study area can be further described with its Geographical Location, Population and Culture, Vegetation, Hydrological condition, Temperature, Salinity, Tide, Colour and water transparency.

D. Location Information

The study area encompasses the city of Port Harcourt's lower reaches. Eagle Island is located between longitudes 7^0 00'E and 7^o 15'E and latitudes 4^0 28'N and 4^0 40'N, and is the southernmost part of Port Harcourt'sBonny River shores. It is a graded beach of the Upper Bonny Estuary in Nigeria's Niger Delta, in the south-central part of the country (Figure 1).

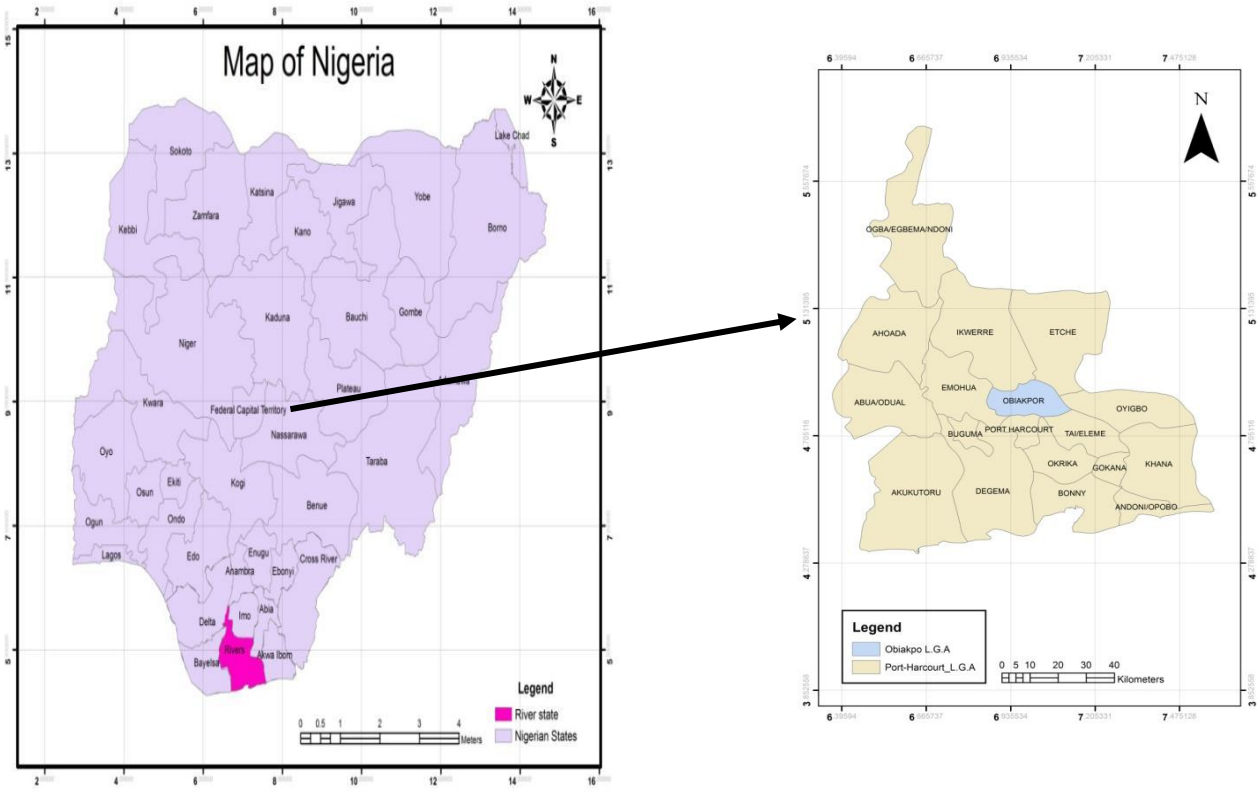

Fig. 1: Map of the Study Area (Jonah and Eke, 2019)

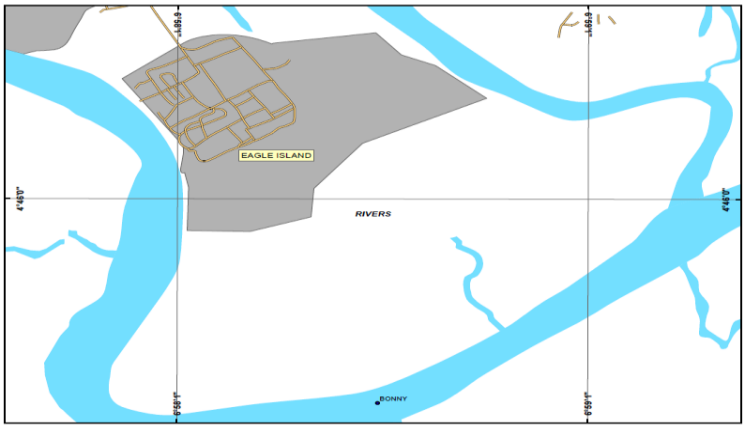

Fig. 2: Map of Nigeria and River state(Jonah and Eke, 2019)

ISSN No:-2456-2165

II. METHODOLOGY

A. *Introduction*

The general work flow diagram is shown (see fig.3). The data and material requirement are discussed and the research stages explained as follows:

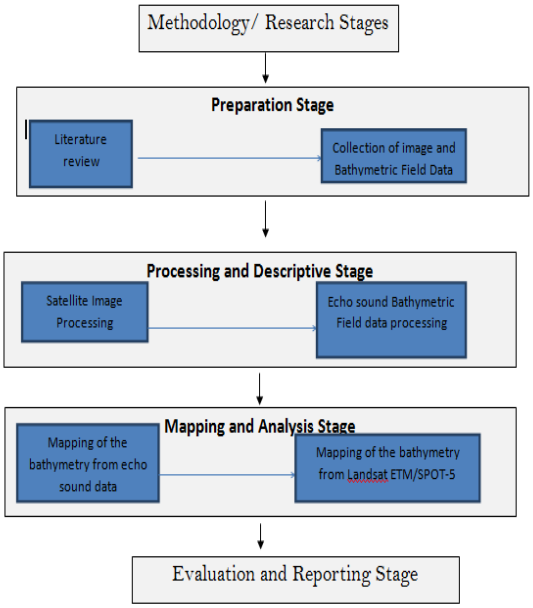

Figure 3.1: Flowchart of the research methodology used.

Fig. 3: Flowchart of the research methodology used

B. *Generated DEM From the Echo Sound Field Data:*

Using Surfer 10.0 software, the data from the field Echo sounding Bathymetric survey was utilized to create a digital elevation model (DEM) of the Eagle Island River.

a) Corrected Satellite Image:
This involves the correction of errors on the images such as:

Radiometric correction is the removal of radiometric errors as a result of effects of sensor sensitivity, and also as a result of the angle of the sun and topography.

Geometric correction is a difference in image coordinates between the actual image coordinates and the ideal image coordinates that would theoretically be projected with an ideal sensor and under ideal conditions. Relief displacement, fluctuations in satellite height and attitude, instrument mis behaviours, and other abnormalities can all cause geometric distortions.

b) Depth Inversion:
As previously indicated, depth inversion techniques entail a series of image processing processes in which the original DN number in the input image is turned into the depth value. The picture processing was done with the ERDAS Imagine software.

c) Image Generation:
The depths generated are used to generate a 3D digital elevation model with surfer 10.0 software. A 3D surface model, contour and wire frame of the Eagle Island was generated, showing the topographic relationship between the river bed and the island.

d) Bathymetric Map:
Bathymetric map of the shore floor showing depth contours is the end product of the entire research produced in paper and soft copy to aid decision making.

C. *Equipment Resource*

Field equipment used for field data collection, are as follows:

- Global Positioning System (GPS)
- Boat
- Midas Digital single beam Echo Sounder
- field sheet

Materials used in this research are as follows:

- Images data LANDSAT ETM+ (1986, 2000 and SPOT 2015)
- Bathymetry map produced from field observation.
- Depth data (In Situ Data)

D. *Software Resource*

Data processing software to be used are as follows:

a) Operating system
Operating system is the platform used to perform data processing and compilation of the results of this thesis writing.

b) ERDAS Imaging and ENVI 4.5
ERDAS software is used to perform the data processing from start to generate absolute depth.

c) Surfer 10 software
Software Surfer 10 is used to perform Kriging interpolation process.

d) Arc GIS 10.7 software
Arc GIS 10.7 software is used to perform the map lay out -making process.

e) Microsoft Excel
Microsoft Excel software is used to perform the calculation processing of data.

f) Microsoft Word
Microsoft Word software used to make the process of typing results thesis.

g) Hydro-CAD software used to process the echo sounding field observation.

ISSN No:-2456-2165

III. DATA ANALYSIS, RESULTS AND DISCUSSIONS

The data analysis and results of the shoreline mapping is divided into five main stages: 3D map generation from Echo sound field data, correction of satellite image, depth inversion, satellite image classification assessment and shoreline change analysis from image overlay. The stages mentioned above area discussed in the following sections:

A. Analysis of in-situ Bathymetric Measurements and 3D map Generation from Echo sound Field Data:

During a field campaign at the location, bathymetric measurements were taken in situ with a single beam echo sounder. At Eagle Island, bathymetric surveys were conducted using a Midas single beam echo sounder (500 kHz) and a Garmin GPS 760SCX. A total of 143 water depth measurements were obtained (see Figure 4 for the locations of the survey points). Raw data were imported into Hydro-CAD software for post processing and result produced in a CSV file format. The CSV file was then imported to Surfer 10 software where the contour map, 3D surface analysis was conducted as shown below. Contour map of Eagle Island was generated through direct sounding to get height measurement of the seabed. Interpolated surface values were used to also generate digital terrain model (DTM) and slope analysis. The depths have eight legendary values which start from + 6 to -14 meters but blue colour which depicts water body ranges from -10 to -13 meters. Sky blue colour adequately stance for the shoreline but ranges from -7 to -10 meters. Results shows that both water body and shoreline change according to difference in height geographically.

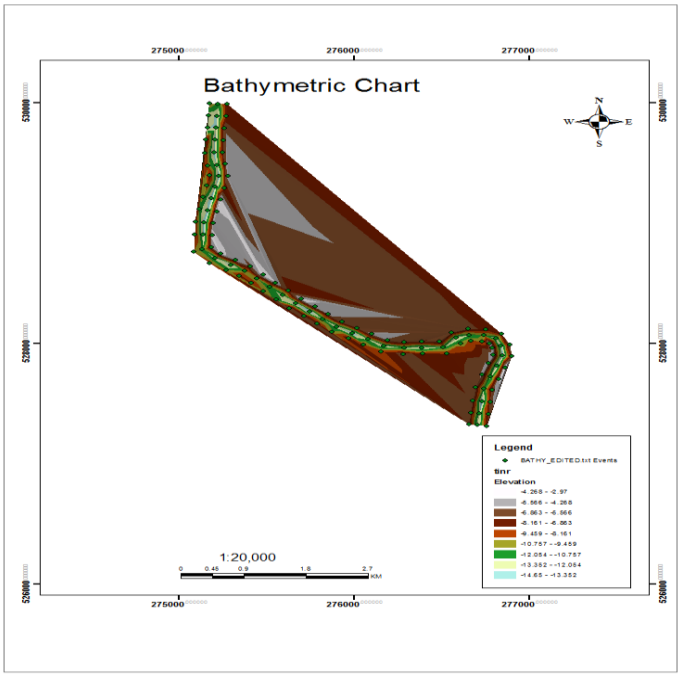

Fig. 4: Bathymetric Chart showing Echo Sound Field Derived Depths with the Elevation shown with different colors on the legend on the bottom Right

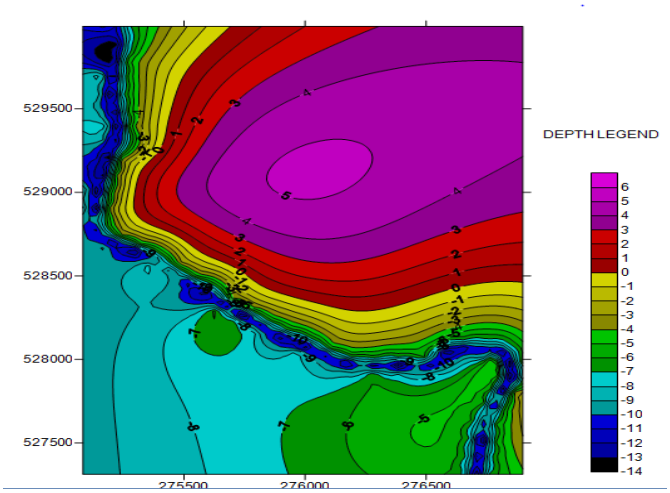

Fig. 5: Contour map generated by the Echo sounding field data using Surfer 10.0 software. The different elevations are shown in different colours. The lowest depth of the river shown on the bottom of the legend and the highest depth of land shown on top

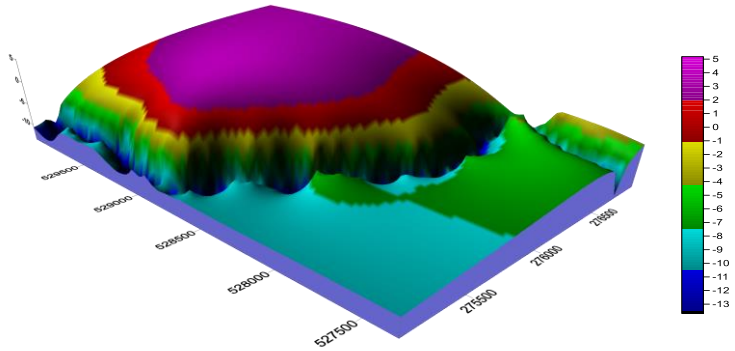

Fig. 6: 3D surface generated by the Echo sounding field data

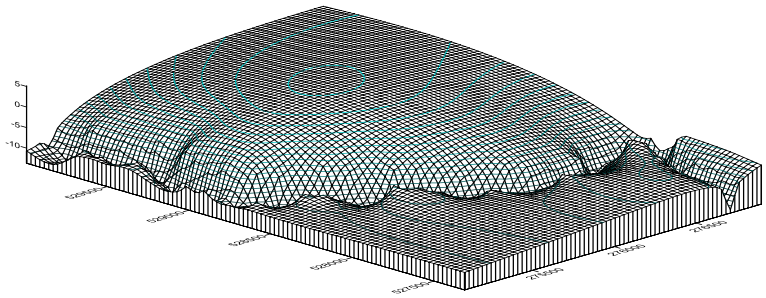

Fig. 7: 3D wire frame generated by the Echo sounding field data

a) 3D Wireframe

The echo sounding data is used to build wireframes, which are three-dimensional representations of a grid file made using Surfer software. Height values are connected along lines of constant eastings (X) and northings (Y) to form a wireframe (Y). Each XY intersection happens at a grid node, and the wireframe's height is proportional to the node's Z value. The amount of X and Y lines drawn on the wireframe is determined by the number of columns and rows in the grid file. This wire frame shows elevation using gradationally coloured lines. The lines' junctions happen at grid nodes.

Figure 7. illustrates the elevation along the Nigeria Agip Oil Company on the west side of the wireframe is between -10 to -12 meters, whereas near the Master Energy and Octopus Nigeria limited have elevation ranging from 0 to -5 meters. This change in depth is as a result of excessive exploration of sand along the Nigeria Agip Oil Company than that of the other area.

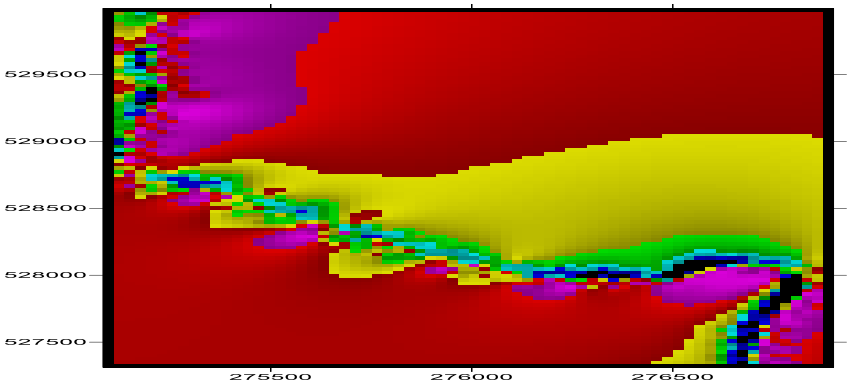

Fig. 8: Shaded relief generated by the Echo sounding field data

A raster map is a shaded relief map. The colours represent the surface's local orientation in relation to a user-defined light source direction. Each grid cell's orientation is determined, and the reflectance of a point light source on the grid surface is calculated. Imagine the sun shining on a topographic surface as the light source. Parts of the surface that are facing away from the light source reflect less light toward the viewer and look darker as a result.

The shaded relief created depicts the many surface relief layers caused by variations in topology elevation.

ISSN No:-2456-2165

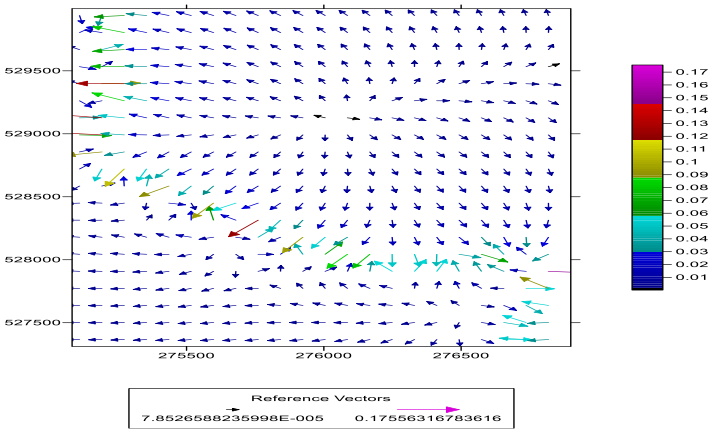

Fig. 9: Vector map generated by the Echo sounding field data showing topographical change

One grid can yield vector map information, including direction and magnitude. The arrow sign indicates that the slope is "downhill," and the length of the arrow is proportional to the slope's magnitude (or steepness). Unless the Frequency setting on the Symbol page in the vector map attributes is changed to skip some grid nodes, a vector is created at each grid node.

Consider the case of a grid having elevation data. The direction arrows would point in the direction water flows if water were poured over the surface - from high elevation to low height. The length of the arrow indicates the magnitude. The steeper slopes in the water flow example would have longer arrows.

B. Correction of Satellite Image

a) Geometric correction for image and chart
To ensure the photograph and the chart are in the equal position, the floor manipulate points measured by way of beacon GPS was used to right the multi-spectral image with an error of less than two pixels, and take the points of intersection of latitude and longitude as controls to right the chart that has been scanned. The corrected image and the corrected chart were well-matched at the same location using the same WGS84 geographic coordinate system, which was then converted to UTM zone 32 North projections.

b) Noise reduction and radiance calculation
The speckle noise exists at the unique photo, and need to be decreased earlier than use. The approach of median filtering (three × three template) is used for de-noise on this paper. Not best it is able to lessen the noise, however additionally it is able to maintain the info of the photo and save you the threshold blurring. The 1A-degree statistics of SPOT-five satellite tv for pc is processed via way of means of radiometric correction primarily, in the procedure of which the pixel value quantified from 0 to 255. Through the calibration of radiation, we can get the radiance of the surface features. The formula is as follows:

$$L=X/A+B \qquad (6)$$

Where L is the radiance that the sensor acquired from the floor features, A is absolutely the calibration-advantage of the radiation-corrected photo, and B is the calibration-bias of the photo. We can get that the parameter A is 1.829788 and B is zero from the PHYSICAL_GAIN and PHYSICAL_BIAS labels within side the metadata file. According to the formulation above, the radiance of the photo may be calculated.

c) Selection and tidal correction of the depth controls
Remote Sensing's water depth inversion is based on a number of factors, including the water depth and the gray value at the same location as the water depth point. Not only throughout the research region, but also at different depth segments, the controls are distributed as uniformly as possible. One hundred and twenty-three (123) sounding locations were found, with water depths ranging from 2 to 15 meters and roughly ten controls in the 1-meter depth interval.

The theoretical datum surface is used to calculate the water depth on the chart. When the image is taken under normal conditions, the value of the instantaneous water depth is greater than that obtained from a chart influenced by tide. The instantaneous water depth, which is the depth from field measurement plus the tidal height, was utilized to create inversion models.

In distinctive feature of the tide desk in 2015, the tidal peak became 1.8m while thephotograph became being shot. The sum of the intensity from chart and the tidal peak became used because the manipulate intensity for inversion. After inversion, subtract the tidal peak from the inversed cost and acquire the real water intensity finally.

C. Depth Inversion

On the basis of the selected controls, the coefficients of the single-band and dual-band models are calculated. During the calculation, a continuous removal of controls with significant residuals is performed, and the inversion model is optimized under the constraint that the controls are spread in distinct depth segments. The inversion parameters are listed in the table below, and figure 10 shows the scatter

ISSN No:-2456-2165

plots of inversed and measured values (the horizontal axis denotes the inversed value, and the vertical axis denotes the measured value).

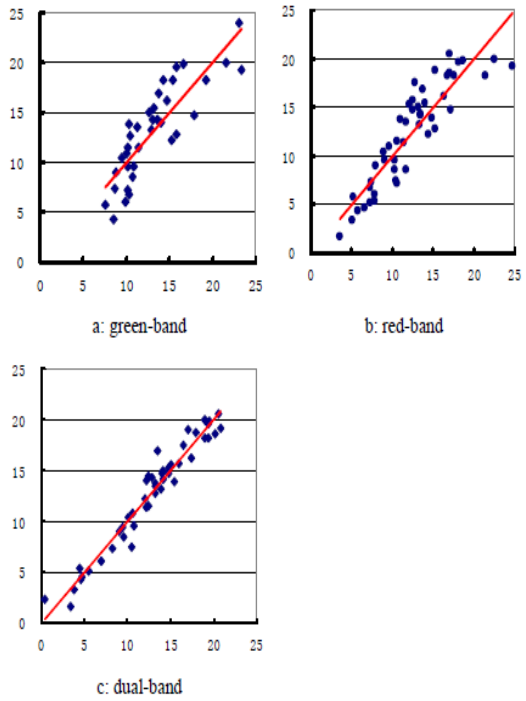

Fig. 10: Scatter Relations of inverse and measured Observation

ERDAS' Model Builder is used to accomplish the inversion procedure. The real water depth is the inverse findings of the three models less the tidal height.

D. Satellite Image Classification Assessment

The assessment of changes in the Eagle Island shoreline requires the analysis of the satellite images. The LandSat ETM -7+ images of 1986, 2000 and SPOT satellite images of 2015 were classified using traditional supervised classification techniques. Arc-GIS 10.1 applications were employed in the classification of the satellite images: ENVI (Environment for Visualizing Images) is ideal software for the visualization, analysis, and presentation of all types of digital imagery. ENVI's complete image-processing package includes advanced, yet easy-to-use, spectral tools, geometric correction, terrain analysis, radar analysis, raster and vector GIS capabilities, extensive support for images from a wide variety of sources, and much more. ENVI's unique approach to image processing combines file-based and band-based techniques with interactive functions. When you open a data input file, its bands are stored in a list where you can access them from all system functions. If you open multiple files, you can process bands of disparate data types as a group. ENVI's interactive analysis capabilities include:

Multiple dynamic overlay capabilities that allow easy comparison of images in multiple displays. Real-time extraction of features area linked spatial/spectral profiling from multi-spectral and hyper spectral data that provide you with new ways of looking at high-dimensional data.

Three classes were selected to analyze the shore line variations from the satellite imageries: vegetation (green), Land use/built-up areas (red) and water bodies (Blue).
And the following assessment analysis was carried out:

a) Error Matrix
The error matrix compares two photographs for the purpose of determining their correctness. It's especially useful for assessing land cover classifications derived from remotely sensed data after they've been classified. The interpreted land cover map is shown on one image, while the ground truth investigation is shown on the other.

ERRORMAT generates an error matrix from these that tabulates the various land cover classes to which ground truth cells have been allocated. In principle, ERRMAT is the same as CROSSTAB, with the distinction that no tabulations are done for cells on the ground truth map marked with a zero. For all classes and per category, the output additionally contains column and row marginal totals, errors of omission and commission, an overall error measure, confidence intervals for that figure, and a Kappa Index of Agreement (KIA).

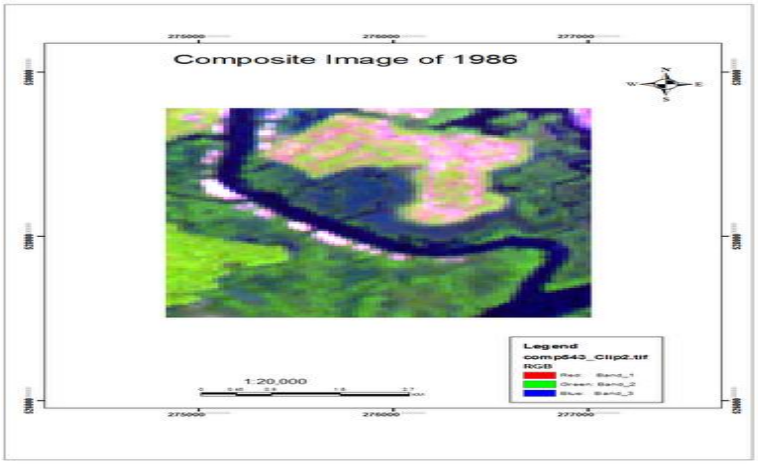

Fig. 11: Composite Map of LandSat 1986 imagery

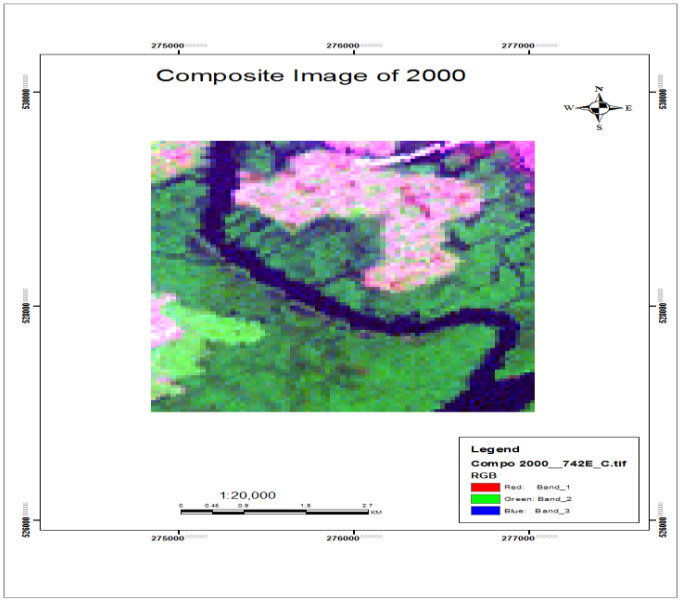

Fig. 12: Composite Map of LandSat 2000 imagery.

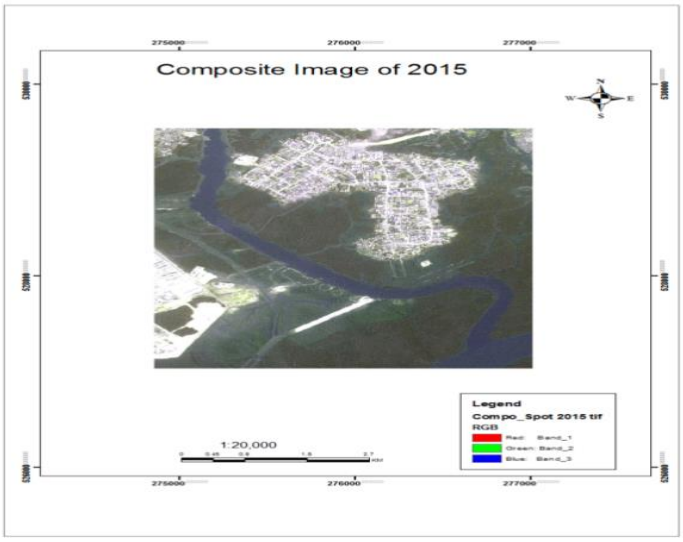

Fig. 13: Composite Map of SPOT 2015 imagery.

b) Confusion Matrix (Pixels)
The confusion matrix is calculated by comparing the ground truth pixel's location and class to the classification image's matching location and class. Each column of the confusion matrix represents a ground truth class, and the values in each column correspond to the ground truth pixels' labeling in the classification image. Built has 691 pixels, water body contained 239 pixels, vegetation has 834 pixels and shoreline embodies 140 pixels. The total Land classification shows 2115 counts while overall Accuracy is 90% and Kappa Coefficient of 85.3%

ISSN No:-2456-2165

Table4. 2: Class Summary for 1986 (Pixels)

Class	Built up	Water Body	Vegetation	Shoreline	Total
Unclassified	0	0	0	0	0
Built up	691	0	11	8	710
Water Body	0	239	1	76	316
Vegetation	0	1	834	64	899
Shoreline	15	8	27	140	190
Total	706	248	873	288	2115

Source: (Author, 2016)

Table 1

Overall Accuracy = (1904/2115) 90.0236%

Kappa Coefficient = 0.8539

c) Confusion Matrix for 1986 (Percent)
The class distribution in percent for each ground truth class is shown in the Ground Truth (Percent) table. The values are determined by dividing the total number of pixels in each ground truth class by the pixel counts in each ground truth column. The class percentage indicate that built up counts 97.88%, water body characterize 96.37%, vegetation brings 95.53% and shoreline showed 48.61%

Table 4.3: Ground Truth for 1986(Percent)

Class	Built up	Water Body	Vegetation	Shoreline	Total
Unclassified	0	0	0	0	0
Built up	97.88	0.00	1.26	2.78	33.57
Water Body	0.00	96.37	0.11	26.39	14.94
Vegetation	0.00	0.40	95.53	22.22	42.51
Shoreline	2.12	3.23	3.09	48.61	8.98
Total	100.00	100.00	100.00	100.00	100.00

Source: (Author, 2016)

Table 2

d) Producer Accuracy
The producer accuracy is a metric that indicates the likelihood that the classifier has classified an image pixel as Class A based on the ground truth. In the case of the confusion matrix, the Built up has a product accuracy of 97.88%, User Accuracy 97.32% and product of 691/706 for ground truth pixels. Shoreline correctly classified 140/288 pixels, producer accuracy 48.61% and User Accuracy of 73.68%.

ISSN No:-2456-2165

Table 4.4: Product/ User Accuracy for 1986

Class	Product Acc. (Percent)	User Acc. (Percent)	Product (Pixels)	User (Pixels)
Built up	97.88	97.32	691/706	691/710
Water Body	**96.37**	**75.63**	239/248	239/316
Vegetation	95.53	92.77	834/873	834/899
Shoreline	48.61	73.68	140/288	140/190

Source: (Author, 2016)

Table 3

e) Omission /Commission

Errors of omission are pixels that belong to the ground truth class but were not classified correctly by the classification procedure. The omission errors are displayed in the confusion matrix's columns. Errors of commission are pixels that are labeled as belonging to the class of interest but actually belong to another class. The commission errors are displayed in the rows of the confusion matrix. Built up reviled commission of 2.68% and omission (2.12%), Water body classified 24.37% in commission and omission of 3.63% with 77/316 pixels. The shoreline classification detailed 26.32% while omission show 51.39%

Table 4.5: Commission/ Omission for 1986

Class	Commission (Percent)	Omission (Percent)	Commission (Pixels)	Omission (Pixels)
Built up	2.68	2.12	19/710	15/706
Water Body	24.37	3.63	77/316	9/248
Vegetation	7.23	4.47	65/899	39/873
Shoreline	26.32	51.39	50/190	148/288

Source: (Author, 2016)

Table 4

Table 4.6: Total Distribution Summary for 1986

Class	Point	Area (M^2)	Percentage (%)
Built up	1113	1,001,700.	17.937
Water Body	661	594,900	10.653
Vegetation	3050	2,745,000	49.154
Shoreline	1381	1,242,900	22.252

Source: (Author, 2016)

Table 5

Compositional data are qualitative descriptors of the whole, conveying exclusive information. Points are also used as real positive numbers, built up contains 1113 points, area of 1,001,700 square meters and 17.937%. Water body exacts 661 points, 594,900 square meters and 10.653%. Vegetation radiant 3050 points show a polygon area of 2,745,000 square meters and 49%. Shoreline in like manner evolves 1381 points, 22% and polygonised to get 1,242,900 square meters.

f) Class Composition for 2000

Table 6 Gives class composition for 2000 Land use classification under which Built up total 804 pixels, water body (315 pixels), vegetation (1004 pixels) and shoreline (225 pixels). 89% was recorded in the overall accuracy and kappa coefficient also recorded 83.5%.

Table 4.7: Ground Truth for 2000 (Pixels)

Class	Built up	Water Body	Vegetation	Shoreline	Total
Unclassified	0	0	0	0	0
Built up	0	0	6	7	804
Water Body	791	255	1	59	315
Vegetation	1	0	937	66	1004
Shoreline	15	19	85	106	225
Total	807	274	1025	238	2348

Source: (Author, 2016)

Table 6

Overall Accuracy = (2089/2348) 88.9693%
Kappa Coefficient = 0.8353

Table 4.8: Ground Truth for 2000(Percent)

Class	Built up	Water Body	Vegetation	Shoreline	Total
Unclassified	0	0	0	0	0
Built up	98.02	0	0.58	2.94	34.24
Water Body	0	93.07	0.10	24.79	13.42
Vegetation	0.12	0	91.06	27.73	42.76
Shoreline	1.86	6.93	8.26	44.54	9.58
Total	100	100	100	100	100

Source: (Author, 2016)

Table 7

Table 7 briefly explained the features classes of the land use for 2000. Percentage is used to discuss the various classes where Built-up reflects 98%, water body 93%, vegetation 91%, and shoreline 44.54%. The result tabulates that Built up has the zenith value 98.02% and shoreline has the least in the composition.

Table 4.9: Commission/ Omission for 2000

Class	Commission (Percent)	Omission (Percent)	Commission (Pixels)	Omission (Pixels)
Built up	1.62	1.98	13/804	16/807
Water Body	19.05	6.93	60/315	19/274
Vegetation	6.67	8.94	67/1004	92/1029
Shoreline	52.89	55.46	119/225	132/238

Source: (Author, 2016)

Table 8

Supervised classification approach was carried out in this section. Four classes were identified on the satellite image using bands 5, 4, and 3 combinations for variable accuracy shown in Table 8 above. Errors of commission are pixels identified as belonging to the class of interest but actually belong to another class. Shoreline under commission is 52.89% while the pixels that belong to the ground truth class but were not classified properly by the classification algorithm are represented by errors of omission. 55.46% falls under omission. Water body is 19.05% for commission and 6.93% for omission.

Table 4.10: Product/ User Accuracy for 2000

Class	Product Acc. (Percent)	User Acc. (Percent)	Product (Pixels)	User (Pixels)
Built up	98.02	98.38	791/807	791/804
Water Body	93.07	80.95	255/274	255/315
Vegetation	91.06	93.33	937/1029	937/1004
Shoreline	44.54	47.11	106/238	106/225

Source: (Author, 2016)

Table 9

Accuracy is the degree to which the result of a measurement, calculation, or specification conforms to the correct value or a standard. According to ISO 5725 'accuracy' is used to describe the closeness of a measurement to the true value. When the term is applied to sets of measurements of the same measuring, it involved component of random error and systematic errors. This means that shoreline is 44.54% in the product accuracy while user accuracy is 47.11%, vegetation shows 937/1029 product pixels and 937/1004 for user pixels in the classification analysis.

Class	Point	Area (M^2)	Percentage (%)
Built up	1,501	1,219,187.2500	21.903
Water Body	766	622,183.5000	11.178
Vegetation	3,145	2,554,526.2500	45.892
Shoreline	1,441	1,170,452.2500	21.027

Table 10: Class Distribution Summary for 2000

Source: (Author, 2016)

g) Ground Truth for 2015

Field Survey is carried out 2015 ground truth exercise, coordinates of selected feature classes were used to train the satellite image. Vegetation, built up, shoreline and water body were identified on the imagery. Built up selected showed 4488 pixels as training samples, vegetation 4673 pixels, water body 3648 pixels and shoreline brought out 816 pixels (Table 11). Overall accuracy is 91% and Kappa coefficient resulted to 87.84%. It will be recalled that (Table 12) clearly showed the needed percentages. Built up is 89.55%, vegetation is 92.66%, water body is 95.77% and shoreline is 77.13%.

Class	Built up	Water Body	Vegetation	Shoreline	Total
Unclassified	0	0	0	0	0
Built up	4488	0	27	65	4580
Water Body	14	3648	1	99	3762
Vegetation	80	0	4673	78	4831
Shoreline	430	161	342	816	1749
Total	5012	3809	5043	1058	14922

Table 11: Ground Truth for 2015 (Pixels)

Source: (Author, 2016)

Overall Accuracy = (13625/14922) 91.3081%
Kappa Coefficient = 0.8784

ISSN No:-2456-2165

Class	Built up	Water Body	Vegetation	Shoreline	Total
Unclassified	0	0	0	0	0
Built up	89.55	0	0.54	6.14	30.69
Water Body	0.28	95.77	0.02	9.36	25.21
Vegetation	1.60	0	92.66	7.37	32.38
Shoreline	8.58	4.23	6.78	77.13	11.72
Total	100	100	100	100	100

Table 12: Ground Truth for 2015(Percent)

Source: (Author, 2016)

Class	Commission (Percent)	Omission (Percent)	Commission (Pixels)	Omission (Pixels)
Built up	2.01	10.45	92/4580	524/5012
Water Body	3.03	4.23	114/3762	161/3809
Vegetation	3.27	7.34	158/4831	370/5043
Shoreline	53.34	22.87	933/1749	242/1058

Table 13: Commission/ Omission for 2015

Source: (Author, 2016)

Four classes were selected to analyze the shoreline variations from the satellite imageries. They are vegetation, built-up, shoreline and water bodies. The error matrix compares two photographs for the purpose of determining their correctness. It's especially useful for assessing land cover classifications derived from remotely sensed data after they've been classified. The interpreted land cover map is shown on one image, while the ground truth investigation is shown on the other. Built up release 2%, 10.45% for omission and 92/4580 pixels, water body brings 3% in the commission, 4.23% for omission and shorelines have 53.34% and 22.87% for both commission and omission for 2015 image analysis.

Class	Product Acc. (Percent)	User Acc. (Percent)	Product (Pixels)	User (Pixels)
Built up	89.99	97.99	4488/5012	4488/4580
Water Body	**95.77**	**96.97**	3648/3809	3648/3762
Vegetation	92.66	96.73	4673/5043	4673/4831
Shoreline	77.13	44.66	816/1058	816/1749

Table 14: Product/ User Accuracy for 2015

Source: (Author, 2016)

User accuracy is a metric that indicates the likelihood that a pixel in a particular class will be correctly classified. Table 14 gives an analysis of the confusion matrix. Shoreline has producer accuracy of 77.13%, user accuracy of 44.66% and the corresponding pixels. In the same vein, built up had producer accuracy of 89.99%, user accuracy of 97.99% with pixel of 4488/5012. Nevertheless, shoreline 77.13% in the producer accuracy, user accuracy of 44.66% and 816/1058 pixels.

Class	Point	Area (M^2)	Percentage (%)
Built up	224,252	1,401,575	25.942
Water Body	70,547	440,918.7500	8.161
Vegetation	336,408	2,102,550	38.916
Shoreline	233,237	1,457,731.2500	26.981

Table 15: Class Distribution Summary for 2015

Source: (Author, 2016)

Class distribution for 2015 is a function in respect of point, area and percentage. Table 15 shows that shoreline characterize 26.981% for the first row, 233237 points and 1457731.250 square meters. Built up obtained 25.94%, 224252 points and 1401575 square meters and Water body gave 8% which give rise to a total of 70,547 points and area of 440918.7500 square meters. In the fourth row, vegetation reveals 38.9%, produced 336,408 points and 2102550 square meters in a polygon form.

E. Image Classification

A minimum of three classes were defined namely built-up areas, water body, vegetation, within the study area.

ISSN No:-2456-2165

a) Application of Supervised Classification

Using the Mahalonobis Distance image classification approach, which employs statistics for each class and is a direction-sensitive distance classifier. It's similar to maximum likelihood classification, except it assumes that all class covariances are the same, making it a faster technique. Unless you set a distance criterion, in which case some pixels may be unclassified if they do not match the threshold, all pixels are categorized to the nearest ROI class. The various defined image classes for the various years were classified as shown in the figures below:

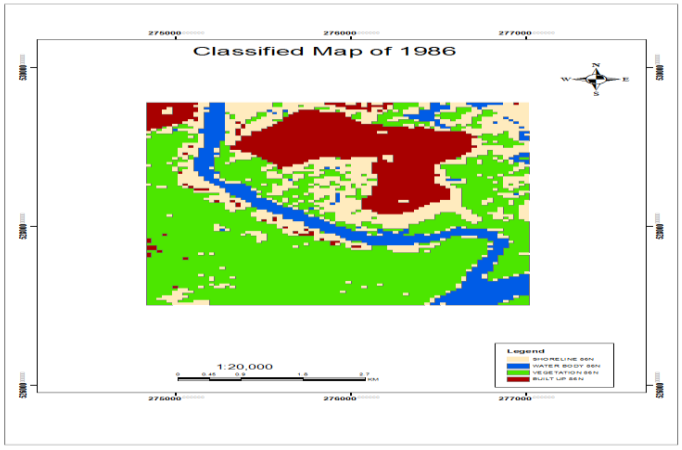

Fig. 14: Classified Landsat image of 1986

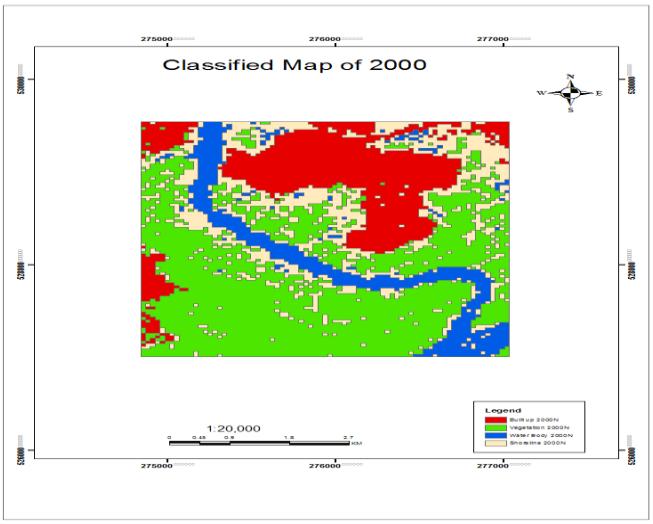

Fig. 15: Classified Landsat image of 2000

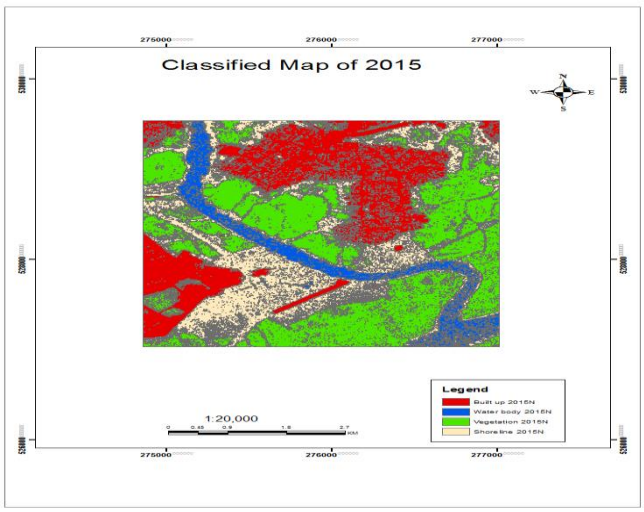

Fig. 16: Classified SPOT image of 2015

ISSN No:-2456-2165

The shoreline for the years 1986, 2000, and 2015 were also identified and obtained from the classified images and shown in Figures below:

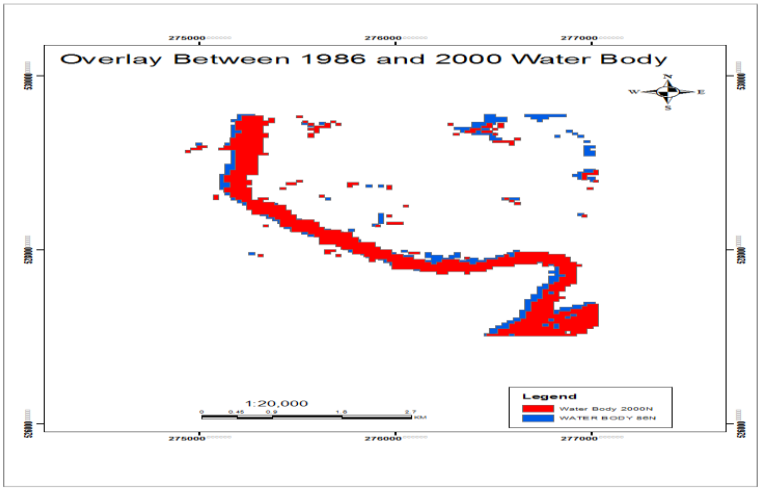

Fig. 17: Overlay between 1986 and 2000 water body

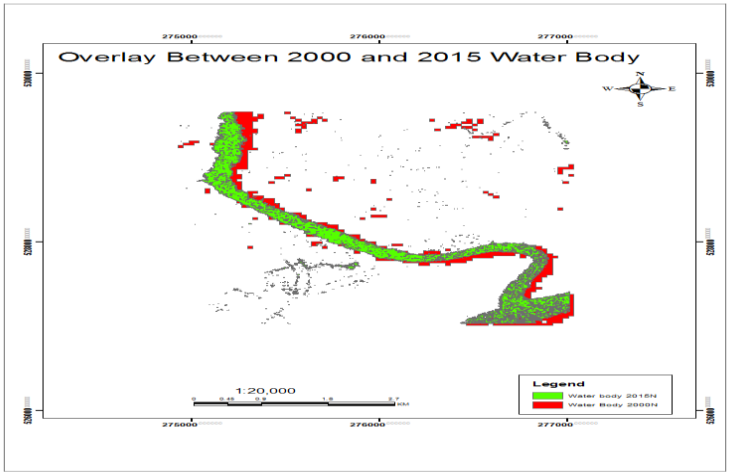

Fig. 18: Overlay between 2000 and 2015 water body

F. Shoreline Changes Analysis from Image Overlay

Beach erosion and accretion are predominant along Eagle Island Communities water ways which were observed during field survey. The presence of Oil Companies such as Nigeria Agip Oil Company and Master Energy NIG., LTD contribute to the problems of shoreline change where their heavy boats along sea routes produces high magnitude of waves to cause accretion and the afore mentioned erosion. Evidence indicates that these areas of the shoreline are experiencing a seasonal reversal in the sand drift along Octopus NIG., LTD over the time past. Thus, shoreline changes call for jetty constructions and other Oil rig plate form to enable exploration and exploitation activities within these areas of operation. It is also wholesome to note that other economic factor which developed sand drift is dredging. Dredging jobs are wide spread in the area under investigation because of its importance in the societal world. However, these operations are examined to bring changes in the shoreline. Figures 4.16 and 4.17Show the field result, along Nigeria Agip Oil Company. Shoreline was defaced by 84 and 77meters between 2000 and 2015. Octopus NIG activities also caused 40- and 62-meters variation along the shore between 2000 and 2015. Master Energy is not farfetched, they contribute to shoreline variation of 54- and 27-meters change within the areas of their operations and the results are model to simulate the shoreline changes that occurred following construction of the jetties and plate form in the river mouth.

a) Overlay Analysis

The shoreline satellite image Spot 2015 was then laid over the shoreline satellite images of 2000, and 1986 and shown in figures 21 and figure 18.

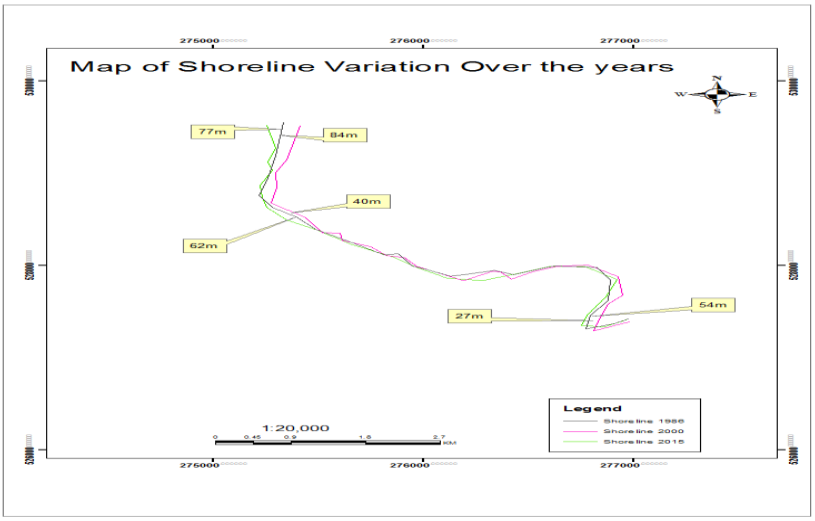

Fig. 19: Map of shoreline variations over the years

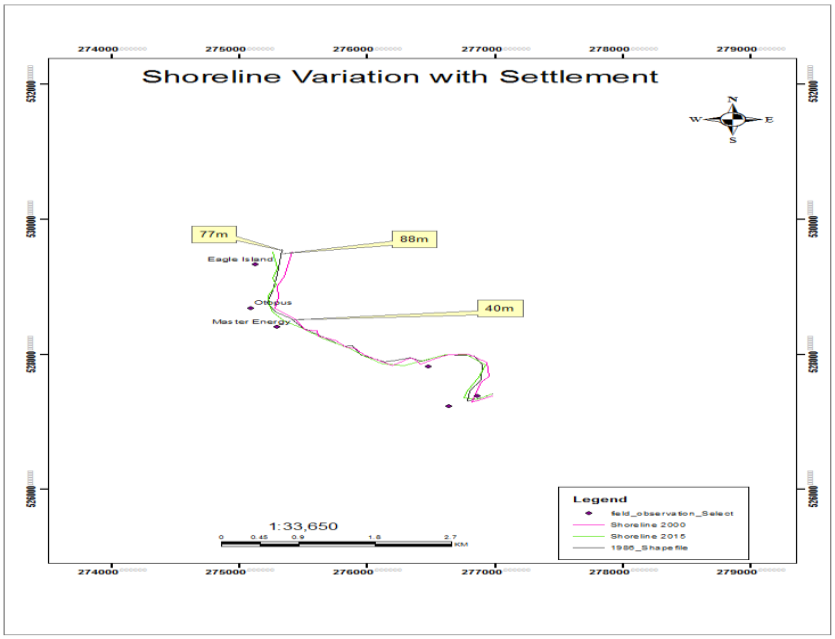

Fig. 20: Map of shoreline variation with settlement

S/No	Year	Lengths of Shoreline (km)
1	1986	3.761
2	2000	3.832
4	2015	3.743

Table 16: Lengths of Shoreline for the years 1986-2015

S/N	Year	Shoreline(M^2)	Shoreline Change(M^2)
1	1986	1,242,900	1,242,900
2	2000	I, 170,452.250	-72447.75
3	2015	1,457,731.250	287279

Table 17: Quantitative Magnitude of Shoreline Change

ISSN No:-2456-2165

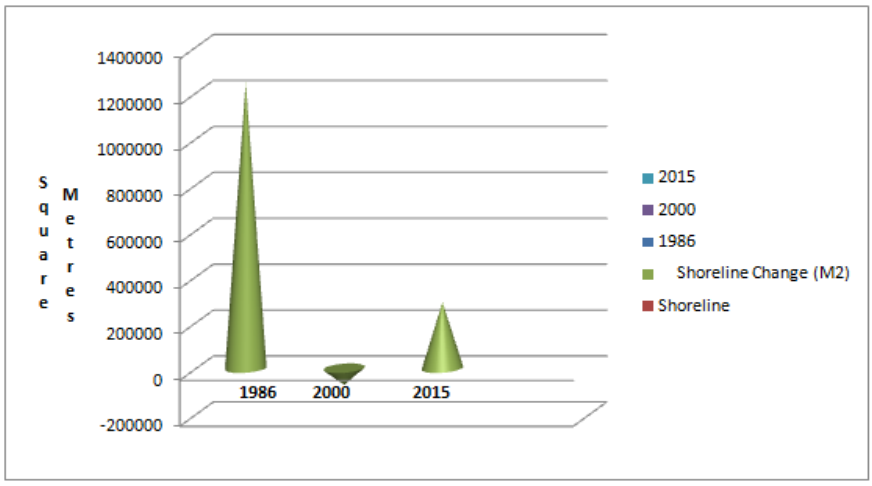

Figure 4.18: Graphical Approach of Shoreline Change

Fig. 21: Graphical Approach of Shoreline Change

Shoreline change is best described in term of graphical approach. Figure 21 expresses the magnitude of change where the vertical alignment represents the unit in square meters while the horizontal axes denote year under investigation. In 1986, the shoreline increases to 1,200,000 Square meters. Decreased was observed in 2000 by -200,000 Square meters along the shoreline, meanwhile in 2015, increase in water level correspondingly led to a positive value above 200000. The result stated here explained that shoreline changes from 1986 to 2015 due to loss of water body.

Class	1986 Area (M^2)	2000 Area (M^2)	2015 Area (M^2)
Built up	1,001,700	1,219,187.2500	1,401,575
Water Body	594,900	622,183.5000	440,918.7500
Vegetation	1,242,900	1,170,452.2500	2,102,550
Shoreline	2,745,000	2,554,526.2500	1,457,731.2500

Table 18: Change Analysis for Land Use/Land Cover between 1986, 2000 and 2015

Source: (Eke & Jonah, 2016)

IV. CONCLUSIONS AND RECOMMENDATIONS

A. *Conclusions*

Landsat ETM-7 + Imageries of 1986 and 2000, and SPOT-5imagery of 2015 were acquired from Glover Land Cover Facility (GLCF), pre-processed and classified using the ENVI 4.5 software. During the study period, 1986-2015, four Land Use/Land Cover (LU/LC) types were found on satellite images. The Garmin-GPS receiver was used to obtain the rectangular co-ordinates of all the points and major features along the shoreline to give the current status of the shoreline in 2015.Satellite images from 1986, 2000, and 2015 were analysed and categorised to indicate the state of the shoreline in those years. After that, the shoreline arrangement in 2015 was compared to satellite images from 1986 and 2000. Infrastructure development, navigation dredging, and reclamation were all common in the study area and had an important role in changing the shoreline. As a result of extensive infrastructure development, there was a considerable loss of mangrove and vegetation inside the study region.

The use of a mix of remote sensing image processing techniques and GIS software to detect shoreline changes over time in relation to economic and social issues has shown to be a unique and crucial tool in detecting shoreline changes over time. It is critical to monitor the shoreline in order to support efficient coastal and shoreline management (Abdullah et. Al 2000).

It's crucial to remember that the capacity to assess the performance of satellite-derived bathymetry models is constrained by the data available for assessment, and that sites with sufficient satellite and field data to allow model creation and assessment are uncommon.

B. *Recommendations*

The following recommendations are hereby put forward:

- By combining tide-linked bathymetric datasets with improved spatial coverage and vertical resolution, much of the inaccuracy in shallow depths might be eliminated.
- This study proposes a solution to the problem of coastline mapping using traditional survey methods.
- Regular mapping of shorelines is needful to avoid costly location of structures along the shore, and to assist with proper boundary definition especially for Riparian communities.

REFERENCES

[1.] Abdullah, K., MatJafri, M.Z. and Din, Z.B. (2000). Contribution from remote sensing in updating bathymetric chart, GIS Development Proceedings,

[2.] www.gisdevelopment.net/aars/acrs/2000/ps3/ps311pf.htm.

[3.] Abdullah, K., MatJafri, M.Z. and Din, Z.B., (2000). Remote sensing of total suspended solids in Penang coastal waters, Malaysia, GIS Development Proceedings, www.gisdevelopment.net/aars/acrs/2000/ps3/ps312.shtml.

[4.] Abdullah, K., MohdDimyata, K., Crackneil, A.P., and Vaghan, R.A., (1991). Evaluation of TM and SPOT data for shallow water Bathymetry, GIS Development Proceedings, www.gisdevelopment.net/aars/acrs/1991/ocean/ocean009.shtml.

[5.] Abu Daya, M.I., (2001). Analysis of multitemporal satellite imagery for total suspended sediments in Coastal waters of Golfito and Golfo Dulce, Costa Rica. ITC-Coastal Zone Studies report.

[6.] Abu Daya, M.I., (2004). Coastal water quality monitoring with remote sensing in (East Kalimantan) Makassar Strait, Indonesia, (unpublished M. Sc. Thesis) International Institute for Geo-Information Science and Earth Observation.

[7.] Bagheri, S., Stein, M. and Dios, R., (1998). "Utility of Hyperspectral data in Bathymetric Mapping in a Turbid Estuary", Int'l Jour. of Remote Sensing, Taylor & Francis Ltd, 1998, Vol. 19, No. 6, 1179-1188.

[8.] Bagheri, S. and Zetlin, C.,(1994). " Bathymetry Mapping with Airborne Imaging Spectrometer Data". 2nd ERIM Thematic Conf. on Remote Sensing for Marine and Coastal Environment, New Orleans, LA., Jan. 1994, Vol. II, pp. 104-111.

[9.] BILKO, (1999). BILKO for windows module 7, lesson 4, UNESCO, pp. 113-120.

[10.] Bukata, R.P., John, H.J., Krill, Y.K. and Dimitry, V.P., (1995). Optical Properties and Remote Sensing of Inland and Coastal waters, CRC Press, USA.

[11.] Campbell, J.B., (1996). Introduction to Remote Sensing, new York: Guilford Publications, Inc., pp. 519-537.

[12.] Anyanwu, C.N. (1971). 'Port Harcourt: 1912-1955 A study in the Rise and Development of a Nigerian Municipality', PhD Thesis, University of Ibadan.

[13.] Das, S.C., (2002). Modern oceanography (in bangle), 2nd edition, Mrs. Esa Das, B-16, Jahangirnagar University, Savar, Dhaka-1342, pp. 335-354.

[14.] Densham, M. P. J. (2005). Bathymetric mapping with Quickbird data.

[15.] Dekker H, Hergi Arst. (1995). Optical Properties and Remote Sensing of Multicomponental Water Bodies.

[16.] Eastman, R.J., 1992, User's Guide, IDRISI, Clark Lab, Massachusetts: Clark University, pp. 119-124.

[17.] Edwards, A., 1999, The Remote Sensing Handbook for Tropical Coastal Management, UNESCO.

[18.] Eludoyin O.S, T Oduore, AA Obafemi 2012, Spatio-temporal analysis of shoreline changes in bonny Island, Nigeria- Ethiopian Journal of Environmental …, 2012 - ajol.info

[19.] Fundamentals of Remote Sensing, (2013). (Canada center for remote sensing tutorial).

[20.] German Aerospace Center, Berlin, Germany, www.ba.dlr.de/NE-WS/ws5.

[21.] Hagan, J., (1998). User's Guide, Cartalinx, Clark Lab, Massachusetts: Clark University, pp. 92-97.

[22.] Izeogu, C.V. (1989). *Environmental Problems in Third World Cities*. International Institute for Environment & Development. p. 60. ISBN 1-84369-072-1.

[23.] Lillesand, T.M. and Kiefer, R. W., (2002). Remote Sensing and Image Interpretation, new York: John Willy & Sons, Inc., , p, 318, 396 and 415.

[24.] Lo, C.P., and Yeung, A.K.W., (2002). Concepts and Techniques of Geographic Information System, New Delhi: Prentice-Hall, Inc., pp. 136-182.

[25.] Louchard, E.M., Pamela Reid, R. and Carol Stephans, F., (2003). Optical remote sensing of benthic habitat and bathymetry in coastal environments at Lee Stocking Island, Bahamas: A comparative spectral classification approach, Limnol. Oceanogr., 48(1, part 2), pp. 511-521.

[26.] Mancebo, F.F., Bruce, R.C., Catalan, Z.B., Lim suan, M.P. and Malayang, B.S., (1997). Correlation of Total suspended Sediments and Reflectance of Landsat TM in Laguna De Bay, Philippines, GIS Development Proceedings, www.gisdevelopment.net/aars/acrs/1997/ts2/ts2003pf.htm.

[27.] Narayan, LRA., (1999). Remote Sensing and it's Application, India: University Press, Ltd., pp. 1-7.

[28.] NaifMuidh Alsubaie.,(2012). The Potential of Using Worldview-2 Imagery for ShallowWater Depth Mapping, (URL:

[29.] http://www.geomatics.ucalgary.ca/graduatetheses)

[30.] Olumide, Fadahunsi, Pe'eri, S., and Armstrong, A. A., "Characterization of the Nigerian Shoreline using Publicly-Available Satellite Imagery", Hydro International, vol. 18(1). pp. 22-25, 2014.

[31.] Okwere O. A, (2015).Portharcourt Shorelne change Mapping and Analysis using Real Time Kinematics (GPS) and Satellite Imageries from 1980-2015.

[32.] Pawlenko, Matthew, (2011). Derivation of river bathymetry using imagery from unmanned aerial vehicles (UAV).http://hdl.handle.net/10945/5466.

[33.] Philpot, W., Analysis of Hyperspectral Data for Coastal Bathymetry and Water Quality, www.opl.ucsb.edu/hycode/pubs/onr01.

[34.] Poonawala, I. Z., Ranade, S. D., Selvan, S., Gnanaseelan, C. and Rajagopalan, A., (1999). Detection of shallow water depth using remotely sensed data, GIS Development Proceedings,

[35.] www.gisdevelopment.net/application/nrm/water/ground/watg0015pf.htm.

[36.] "Rivers Population Statistics". City Population.de. Retrieved 7 September 2016.

[37.] Shanwei Liu JieZhang , Yi Ma,Yantai, (2010). Bathymetric Ability of SPOT-5 Multi-Spectralimage in shallow coastal water,Institute of Coastal Zone

Research, Chinese Academy of Sciences, Yantai, China.
[38.] Vanderstraete ,T.K. Ghabour, R. Goossens, (2002).Bathymetric Mapping of Corel Reefs in the Red Sea.Presented at the Seventh International Conference on Remote Sensing for Marine and Coastal Environments, Miami, Florida, 20-22 May 2002.
[39.] Vathananukij, H., Murai, S., Vibulsresth, S., Katsumi, M., Ryosuke, S., Kakiuchi, H., Yasuoka, Y., and Yamakata, Y., (1994). Water Quality Analysis on the Chao-Phra-Ya Estuary Using Remote Sensing Data, GIS Development Proceedings, www.gisdevelopment.net/aars/acrs/1994/ts2/ts2006pf.htm.
[40.] Wong P.P, R. J. Nicholls, P. P.(2007)."Coastal systems and low-lying areas"understanding of the implications of climate change for coastal systems and low-lying areas.2007 - ro.uow.edu.au. Abstract Since the IPCC Third Assessment Report (TAR)
[41.] www.csc.noaa.gov/products/nchaz/htm/ccap5.htm. (2015)
[42.] www.marine.usf.edu/geology/ccom.html. (2015)
[43.] www.obee.ucla.edu/test/faculty/nezlin/RemoteSensingOfTheSea.htm. (2015)